

# A Photoinitiator-Free Photosensitive Polyimide with Low Dielectric Constant

Seunghyuk Choi,<sup>1</sup> Seokkyu Lee,<sup>1</sup> Jihee Jeon,<sup>1</sup> Jaemin An,<sup>1</sup> Sher Bahadar Khan,<sup>1</sup> Sangyup Lee,<sup>1</sup> Jongchul Seo,<sup>2</sup> Haksoo Han<sup>1</sup>

<sup>1</sup>Department of Chemical Engineering, Yonsei University, 134 Shinchon-dong, Seodaemun-gu 120-749, Seoul, Korea

<sup>2</sup>Department of Packaging, Yonsei University, 234 Maeji-ri, Heungup-myun, Wounju-si 220-710, Gangwon-do, Korea

Received 15 July 2009; accepted 2 February 2010

DOI 10.1002/app.32213

Published online 27 April 2010 in Wiley InterScience (www.interscience.wiley.com).

**ABSTRACT:** A series of photoinitiator-free photosensitive polyimides (PSPIs) with lower dielectric constants have been synthesized by reaction of fluorine aromatic diamine, 2,2'-bis(3-amino-4-hydroxyphenyl)hexafluoropropane diamine (AHHFP) with 3,3',4,4'-benzophenonetetracarboxylic dianhydride (BTDA) and a mixture of various mole ratios of 3,3',4,4'-benzophenonetetracarboxylic dianhydride (BTDA) and 4,4'-(hexafluoroisopropylidene)diphthalic anhydride (6FDA) by using solution polycondensation reaction at room temperature and further imidization at 180°C. These aromatic polyimides were further acrylated via a reaction with acryloyl chloride in the presence of triethyl amine to produce negative photoinitiator-free PSPIs. All the photoinitiator-free photosensitive

polyimides were characterized by FTIR and NMR while their morphology was evaluated by X-ray diffractions study. These newly synthesized PSPIs were evaluated to determine their electrical, thermal, and photolithographic properties. The PSPI (AHHFP-BTDA-6FDA [1 : 0.5 : 0.5]) with high mole ratio of 6FDA showed lower dielectric constants of 2.420 at 1 kHz and 2.170 at 1 MHz in capacitance and optical methods, respectively. Further, the acrylated AHHFP-BTDA showed the highest photosensitivity than other PSPIs. © 2010 Wiley Periodicals, Inc. *J Appl Polym Sci* 117: 2937–2945, 2010

**Key words:** photosensitive polyimide; photoinitiator-free; dielectric constant

## INTRODUCTION

Aromatic polyimides possess outstanding thermal, mechanical, and electrical properties as well as excellent chemical resistance, which explains that their large use in domains, such as electronics and aerospace industry.<sup>1,2</sup> However, much attention is needed to develop thermally stable polyimides with improved solubility and low dielectric constants for high-speed and high-frequency circuit applications.<sup>3</sup> Most of the polyimides strongly absorb visible light, and have relatively higher dielectric constants  $\epsilon$  over 3.0.<sup>4</sup> Also polyimides are somewhat difficult to be fabricated because of their infusibility and insolubility in some organic solvents. One approach to overcome these shortcomings without sacrificing the thermal and mechanical properties is to introduce flexible functional groups in the polymer backbone, low molar polarization atoms per molecular volume, bulky structures, low orientated structures in the PI

backbones, and lower-electron density structures such as electron-withdrawing units or aliphatic moieties to PI backbone.<sup>2</sup>

Recently, photosensitive polyimides (PSPIs) have attracted a great interest because they simplify the processing steps by avoiding the use of any photore-sist to obtain the desired patterns.<sup>5,6</sup> Generally, in the most photosensitive polyimide systems, low molecular weight photoinitiators are needed.<sup>7,8</sup> In fact, only a little part of photoinitiators can be used in illumination process, resulting in a large amount of photoinitiator residues, which leads to decrease the thermal, mechanical, and electrical properties of the PSPIs. Therefore, photoinitiator-free photosensitive polyimides are highly desired to overcome this problem.<sup>9–11</sup>

We choose a bulky CF<sub>3</sub> substituted anhydride because the incorporation of symmetric fluorinated substituents into polymers can be reduced in relation to the mutual repulsion of the outermost shell electrons of fluorine atoms, the relatively small dipole of C-F bonds, and the large free volume of trifluoromethyl groups, which results in low intermolecular cohesive energy and low chain packing efficiency. A large number of fluorine-containing polyimides have been reported because of their excellent heat resistance, reduced coloration, and lower moisture absorption and  $\epsilon$  values.<sup>12</sup>

Correspondence to: H. Han (hshan@yonsei.ac.kr).

Contract grant sponsor: National Research Foundation of Korea Grant funded by the Korean Government (MEST); contract grant number: NRF-2009-C1AAA001-0092926.

In this study, the fluorine aromatic diamine, 2,2'-bis(3-amino-4-hydroxyphenyl)hexafluoropropane diamine (AHHFP) was selected to polymerize with 3,3',4,4'-benzophenonetetracarboxylic dianhydride (BTDA). Furthermore, for lower dielectric constants, a series of co-polyimides were also synthesized from the AHHFP, BTDA and another dianhydride, 4,4'-(hexafluoroisopropylidene)diphthalic anhydride (6FDA) which has the bulky  $\text{CF}_3$  group by the method of solution polycondensation at room temperature and imidized at a high temperature to get hydroxyl polyimides. Then these hydroxyl polyimides were acrylated by acryloyl chloride to obtain negative photoinitiator-free PSPIs. These PSPIs were subjected to solubility, optical, dielectric property, and thermal measurements.

## EXPERIMENTAL

### Materials

Acryloyl chloride and *r*-valerolactone were purchased from TCI and used as received. 3,3',4,4'-Benzophenonetetracarboxylic dianhydride (BTDA, Aldrich) was recrystallized from acetic anhydride and dried in a vacuum oven at 120°C for 10 h before using. 4,4'-(Hexafluoroisopropylidene) diphthalic anhydride (6FDA, TCI) and 2,2-bis(3-amino-4-hydroxyphenyl)hexafluoropropane (AHHFP, TCI) were used without further purification. *N,N'*-dimethylacetamide (DMAc) and *N*-methyl-2-pyrrolidone (NMP) were

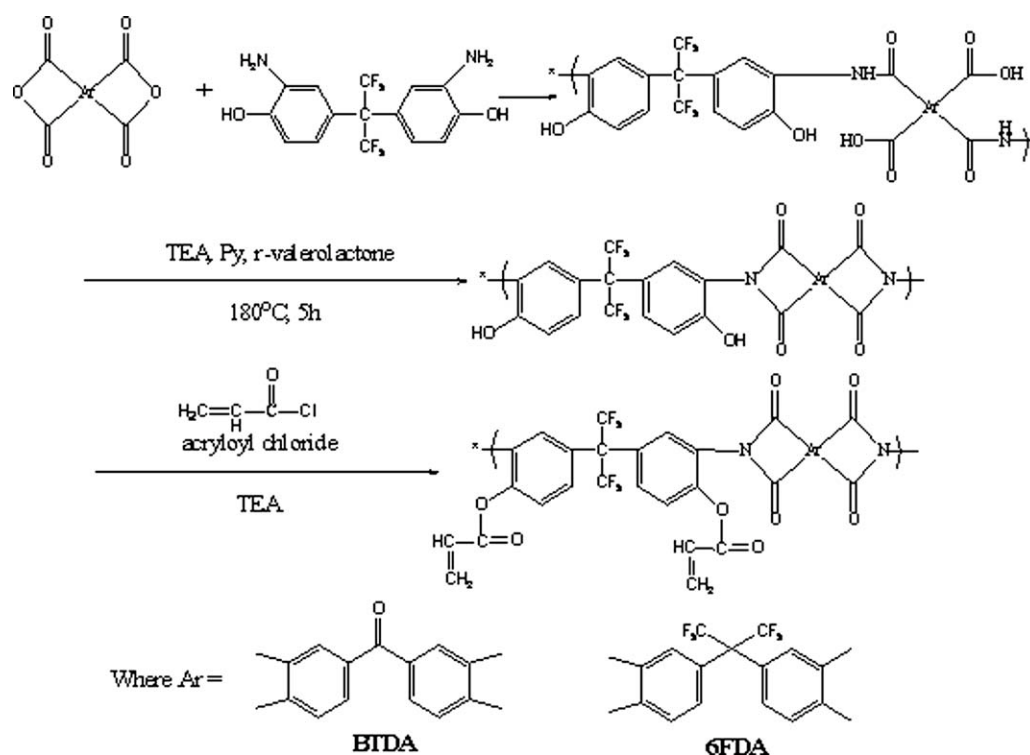
purified by distillation under reduced pressure from calcium hydride before use.

### Synthesis of hydroxyl polyimide

AHHFP (5 mmol) and TEA (1 mmol) were placed in 250-mL three-necked round bottom flask, fitted with a Dean-Stark trap and condenser, followed by the addition of mixed solvent of NMP/toluene (12.5/4 mL) in that flask. After the mixture was completely dissolved, BTDA (5 mmol), *r*-valerolactone (1 mmol), and pyridine (1 mmol) were added into the solution. Then the mixture was kept at 180°C for 5 h under nitrogen flow. After cooling to the room temperature, 12.5 mL of NMP was added to the mixture and then it was precipitated in methanol/water (volume ratio 1 : 1). The hydroxyl polymer was collected by filtration and washed several times with fresh methanol, and dried in vacuum oven at 80°C for 24 h. The white-to-grayish polyimide powder was obtained in quantitative yield (3 g, 4.6 mmol, 92%). In addition, the co-polyimides were also prepared from the AHHFP (5 mmol) - BTDA (3.5 mmol) - 6FDA (1.5 mmol) and AHHFP (5 mmol) - BTDA (2.5 mmol) - 6FDA (2.5 mmol) as the same previous method. The quantitative yields are 86.8% and 85.2% for AHHFP-BTDA-6FDA (1 : 0.7 : 0.3) and AHHFP-BTDA-6FDA (1 : 0.5 : 0.5) respectively.

### Synthesis of photoinitiator-free PSPI

Each hydroxyl polyimide (3.01 mmol of the repeating unit) was dissolved in 20 mL of NMP in a



Scheme 1 Scheme and chemical structure of PSPI.

250-mL three-necked round bottom flask equipped with a condenser and a nitrogen inlet and an excess amount of acryloyl chloride (6, 9, 12 mmol per hydroxyl repeat unit) already dissolved in 20 mL NMP and TEA (the same amount of acryloyl chloride) was added in each hydroxyl polyimide solution under nitrogen atmosphere. The mixture was stirred at different allocated time intervals and then poured into 1000 mL of methanol to remove triethylammonium chloride. The precipitate was filtered and washed several times with fresh methanol and dried in vacuum oven at 80°C for 24 h.

### Preparation of PSPI patterns

The PSPI was dissolved in DMAc at a solid content of 10 wt %. The films were prepared via spin coating on clean silicon substrates and prebaked at 80°C for 2 h. The thickness of films was about 2  $\mu\text{m}$ . The photoresist film was exposed in the contact mode with a mask to a low pressure mercury UV (365–436 nm) with UV dose of 1400  $\text{mJ}/\text{cm}^2$ . The film was then developed in a mixture of DMAc/2-propanol (volume ratio 5 : 1) for 3 min and rinsed with 2-propanol. After development, the films were dried at 80°C for 2 h.

### Measurements

$^1\text{H-NMR}$  was analyzed by using Varian Mercury INOVA 500 MHz  $^1\text{H}$  spectrometer. Fourier transform infrared (FTIR) spectra of the polyimides were obtained with a Tensor 27 (Bruker Co.) instrument from 650 to 4000  $\text{cm}^{-1}$  on KBr pellets. The diffractometer was set up for the reflection mode (i.e., reflections from lattice planes parallel to the film surface).  $\text{CuK}\alpha$  radiation source ( $\lambda = 1.54 \text{ \AA}$ ) was operated at 40 kV and 40 mA. All the WAXD measurements were carried out in the  $\theta/2\theta$  mode. The details are described in our previous studies.<sup>13,14</sup>

DSC analyses were performed on a TA Instruments DSC Q10 in flowing nitrogen at a heating rate of 10°C/min. Thermo gravimetric analysis (TGA) thermograms of polyimides were obtained with a thermo gravimetric analyzer (TA Instruments Co., United States) from 25 to 800°C at a heating rate of 10°C/min. The coefficient of thermal expansion (CTE) was measured using a thermomechanical analyzer. TMA (TA instrument, Q-400) was measured at a heating rate of 10°C/min from 30°C to 400°C in nitrogen. All of these thermal properties measured in  $\text{N}_2$  atmosphere.

The dielectric properties of polyimides were measured by the capacitance method and optical method. The dielectric measurements of polyimide thin films were monitored at room temperature and 1 kHz with a Fluke PM6304 thin film dielectric analyzer.<sup>15</sup>

A sample was placed inside a chamber that isolated the sample from the outside ambient relative humidity and temperature. The capacitance was recorded at room temperature. The dielectric constant ( $\epsilon'$ ) by the capacitance method was calculated from the measured capacitance data as follows.

$$\epsilon' = \frac{CL}{\epsilon_0 A}$$

where  $C$  is the capacitance,  $\epsilon'$  is dielectric constant,  $\epsilon_0$  is the permittivity of free space ( $8.854 \times 10^{-12} \text{ F/m}$ ),  $L$  is the film thickness, and  $A$  is the electrode area.

For the determination of the dielectric constant by the optical method, the out-of-plane and in-plane refractive indices of the polyimide thin films were measured with a prism coupler (model 2010, Metricon) equipped with a He-Ne laser light source (wavelength = 632.8 nm) and controlled by a computer. The measurements of the refractive indices were carried out in both transverse electric (TE) and transverse magnetic (TM) modes with the appropriate polarization of the incident laser beam, as described elsewhere.<sup>16</sup> The TE measurement in which the electric field was in the film plane provided the in-plane refractive index, whereas the TM measurement in which the electric field was out-of-plane gave the out-of-plane refractive index.

Ultraviolet-visible (UV-vis) spectra of the polymer films were recorded on an Agilent UV-visible spectroscopy. Surface profiler ( $\alpha$ -step) was used to measure film thickness for photosensitivity and the lithographic performance of a PSPI was investigated with JEOL-5410LV scanning electronic microscope (SEM).

## RESULTS AND DISCUSSION

### $^1\text{H-NMR}$ spectrum

The PSPIs were synthesized through two step processes. The hydroxyl PIs were prepared through polycondensation in the presence of the catalyst systems of *r*-valerolactone and pyridine. In the  $^1\text{H-NMR}$  analysis, the signal at 10.51 ppm ( $H_a$ ) of the  $^1\text{H-NMR}$  spectrum indicates the hydroxyl group of polyimide. The  $H_a$  was close to the hydroxyl group appeared at the farthest downfield region. Because proton of  $-\text{OH}$  has low electron density. The signals at 8.24 ppm ( $H_g$ ), 8.15 ppm ( $H_{e,f}$ ) determined by effects of  $\text{C}=\text{O}$  group and aromatic ring.  $\text{C}=\text{O}$  group is electron acceptor. So the aromatic protons nearby  $\text{C}=\text{O}$  group have low electron density than others. 7.48–7.05 ppm ( $H_d$ ,  $H_c$ ,  $H_b$ ) shifted to the upfield region due to the electron donating  $\text{CF}_3$  group and  $H_b$  shifted to the downfield region than

$H_c$ ,  $H_d$  owing to the hydroxyl group.  $H_d$  shifted to the downfield region than  $H_c$  because of nitrogen group. Through acrylation of hydroxyl group in hydroxyl PIs, acrylate group can be easily introduced into polyimide side-chain to obtain photoinitiator-free PSPI. The hydroxyl group (10.51 ppm) disappeared while the new acrylate group (6.40–6.02 ppm) appeared as degree of substitution. The degree of acrylation is defined as the number of acrylate groups per repeat unit and is calculated by a comparison of the proton integration values of  $\text{CH}=\text{CH}_2$  protons at 6.40–6.02 ppm. The degree of acrylation was determined by the amount of acryloyl chloride and TEA, reaction time and temperature. The results are summarized in Table I. All of the segments in the PSPI-5 were substituted with acrylate groups and this  $^1\text{H-NMR}$  spectrum is shown in Figure 1. The suitable conditions of acrylation were room temperature, long reaction time over 72 h and the proper amount of each acryloyl chloride and TEA is 9 mmol respectively per hydroxyl repeat unit.

### FTIR spectrum

The structure of polyimide was confirmed by FTIR as shown in Figure 2. The characteristic absorption bands of the imide ring were observed near  $1776\text{ cm}^{-1}$ ,  $1717\text{ cm}^{-1}$  (asymmetrical and symmetrical  $\text{C}=\text{O}$  stretching vibration),  $1371\text{ cm}^{-1}$  ( $\text{C}-\text{N}$  stretching vibration),  $1671\text{ cm}^{-1}$  ( $\text{Ar}_2-\text{C}=\text{O}$  stretching) and  $1100\text{--}1300\text{ cm}^{-1}$  showed some stronger peaks ( $\text{C}-\text{O}$  and  $\text{C}-\text{F}$  stretching).

Through acrylation of hydroxyl group in hydroxyl PIs, acrylate group can be easily introduced into polyimide side-chain to obtain photoinitiator-free PSPI. The acrylated group was observed at  $1403\text{ cm}^{-1}$  ( $\text{C}=\text{C}$  stretching).

### Solubility

The solubility of synthesized fluorinated polyimides was tested in various organic solvents, and the results are summarized in Table II. The solubility behavior of the PIs depended on their chain packing

**TABLE I**  
Relationship of the Acrylation Ratio and the Reaction Conditions

	Acryloyl chloride (mmol)	TEA (mmol)	Temperature ( $^{\circ}\text{C}$ )	Time (h)	Degree of substitution
PSPI-1	6	6	25	24	0.10
PSPI-2	9	9	25	24	0.35
PSPI-3	12	12	25	24	0.40
PSPI-4	9	9	25	36	0.58
PSPI-5	9	9	25	72	1.00
PSPI-6	9	9	60	24	0.10

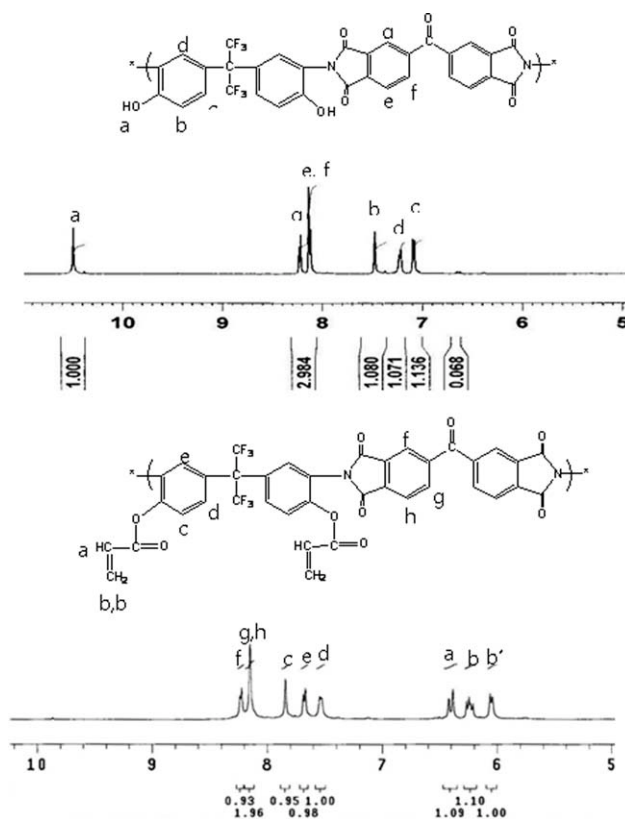


**Figure 1**  $^1\text{H-NMR}$  spectra of hydroxyl PI and acrylated PI.

density and intermolecular interactions. All polyimides were soluble in most solvents. It could be because the diamines with  $\text{CF}_3$ , hydroxyl group and ether group showed great effects, which could inhibit close packing and reduced the interchain

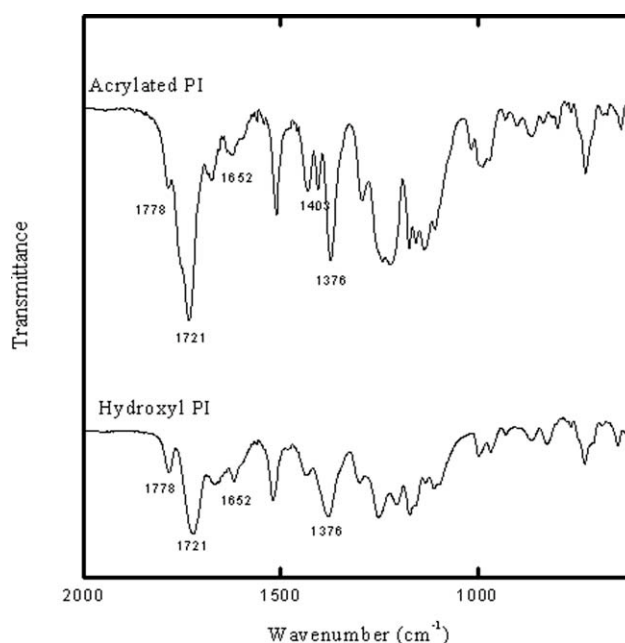


**Figure 2** FTIR data of hydroxyl PI and acrylated PI.

TABLE II  
Solubility Behavior of Polyimides

Polyimide <sup>a</sup>	Solvents <sup>b</sup>							
	NMP	DMAc	DMF	DMSO	Py	THF	MC	Ac
A-B (1 : 1)	O	O	O	O	O	O	X	O
A-B-F (1 : 0.7 : 0.3)	O	O	O	O	O	O	X	O
A-B-F (1 : 0.5 : 0.5)	O	O	O	O	O	O	X	O
Acrylated A-B (1 : 1)	O	O	O	O	O	O	O	O
Acrylated A-B-F (1 : 0.7 : 0.3)	O	O	O	O	O	O	O	O
Acrylated A-B-F (1 : 0.5 : 0.5)	O	O	O	O	O	O	O	O

Qualitative solubility was determined with 10 mg of polymer in 1 mL of solvent.

S (soluble at room temperature); IS (insoluble even on heating).

<sup>a</sup> A, AHHFP; B, BTDA; F, 6FDA.

<sup>b</sup> DMSO, dimethylsulfoxide; Py, pyridine; THF, tetrahydrofuran; MC, methylen chloride; Ac, Acetone.

interactions to enhance solubility. Also, PSPI exhibited better solubility in methylen chloride (MC) than PIs. It might be because the acryloyl group increased the interchain interactions to enhance solubility in MC.

### Thermal properties

The thermal properties of the polyimides were evaluated by means of thermogravimetry analysis (TGA) and dynamic mechanical thermal analysis (DSC). In thermogravimetry analysis, the thermal degradation values at 5% ( $T_5\%$ ) and 10% ( $T_{10}\%$ ) weight loss are given in Table III and Figure 3. Generally, all the PIs and PSPIs have good thermal stability and it increased as the amount of  $CF_3$  increased due to its strong bonding strength. In the comparison of PIs and PSPIs, PSPIs have lower  $T_g$  and thermal degradation values than PIs due to the acrylate group.  $T_5\%$  for PIs and PSPIs ranged from 409.18°C to 421.35°C and 293.51°C to 304.03°C while  $T_{10}\%$  ranged from 443.78°C to 459.87°C and 340.63°C to 351.05°C, respectively.

The glass transition temperatures ( $T_g$ ) of PIs and PSPIs were evaluated by DSC and the values are given in Table III. The  $T_g$  values obtained from DSC

TABLE III  
Thermal Properties of Polyimides

Polyimide <sup>a</sup>	Thermal properties		
	$T_g^b$ (°C)	$T_5\%^c$ (°C)	$T_{10}\%^d$ (°C)
A-B (1 : 1)	322.68	409.18	443.78
A-B-F (1 : 0.7 : 0.3)	359.82	415.19	451.12
A-B-F (1 : 0.5 : 0.5)	365.69	421.35	459.87
Acrylated A-B (1 : 1)	250.25	293.51	340.63
Acrylated A-B-F (1 : 0.7 : 0.3)	254.47	296.36	343.38
Acrylated A-B-F (1 : 0.5 : 0.5)	261.42	304.03	351.05

<sup>a</sup> A, AHHFP; B, BTDA; F, 6FDA.

<sup>b</sup> Measured by DSC.

<sup>c</sup> Temperature at 5% weight loss.

<sup>d</sup> Temperature at 10% weight loss.

ranged from 322.68°C to 365.69°C and 250.25°C to 261.42°C. The polymers containing more  $CF_3$  moieties showed a high  $T_g$  value which may be attributed to the increased polarity of the  $CF_3$  moiety in the polymer backbone. The high  $T_g$  is the result of the increasing order of rigidity and polarity of the polymer chains.<sup>17</sup> These results prove that these polymers can be applied for high temperature applications.

### Dielectric constants

The dielectric constants for the polyimide thin films were evaluated by capacitance method and optical method, respectively, and the values are summarized in Table IV. For comparison with dielectric properties, the dielectric constant by optical method was taken in the perpendicular direction of the film orientation. A similar trend of variation in dielectric

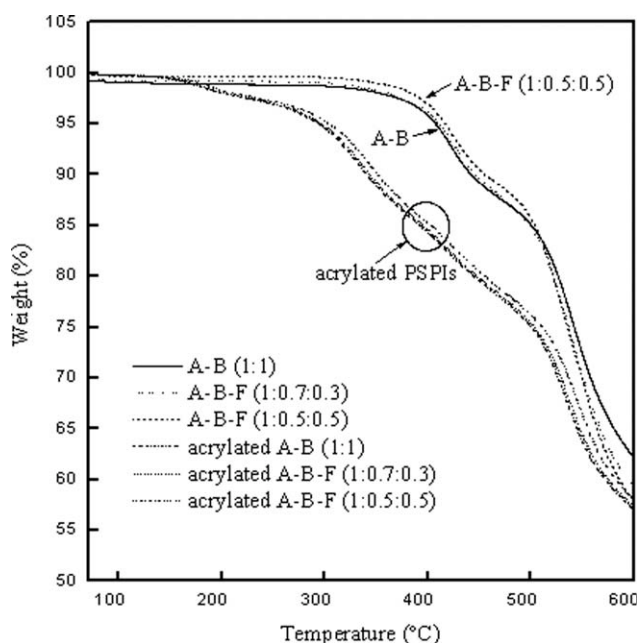


Figure 3 TGA thermograms of hydroxyl PI and PSPI.

TABLE IV  
Dielectric Constants of Polyimides

Polyimide <sup>a</sup>	Capacitance method		Optical method			
	$\epsilon'$ (1 kHz)	$n_{TE}$ <sup>b</sup>	$n_{TM}$ <sup>c</sup>	$n_{ave}$ <sup>d</sup>	$n_{TE} - n_{TM}$	$\epsilon'^e$ (1 MHz)
Acrylated A-B (1 : 1)	2.724	1.5172	1.5149	1.5161	0.0023	2.230
Acrylated A-B-F (1 : 0.7 : 0.3)	2.565	1.5168	1.4768	1.4968	0.0400	2.240
Acrylated A-B-F (1 : 0.5 : 0.5)	2.420	1.4751	1.4690	1.4721	0.0061	2.170

<sup>a</sup> A, AHHFP; B, BTDA; F, 6FDA.

<sup>b</sup> Measured in the transverse electric (TE) mode.

<sup>c</sup> Measured in the transverse magnetic (TM) mode.

<sup>d</sup> Average refractive index,  $n_{ave} = (2n_{TE} + n_{TM})/3$ .

<sup>e</sup>  $\epsilon' = n_{ave}^2$ .

constants by the capacitance and optical method was obtained, but the dielectric constants by capacitance method were higher than values by optical method in all the cases. In the capacitance method, the electronic and nuclear polarizability contributes to the overall dielectric constant whereas in the optical method which the electronic polarizability contributes. Hence, the dielectric constants obtained by the capacitance method are always higher than values by the optical method.<sup>18,19</sup>

Dielectric constant  $\epsilon$  of the material can be estimated roughly from the averaged refractive index  $n$  according to the Maxwell's equation,  $\epsilon = n^2$ . Therefore, the low refractive index materials exhibit low  $\epsilon$ . All the composite films showed larger  $n_{TE}$  than  $n_{TM}$  which indicates that polymer chains are preferentially aligned in the film plane, resulting in positive birefringence ( $\Delta = n_{TE} - n_{TM}$ ) in the composite films.<sup>1</sup> With an increase in the 6DFA content, the  $n_{TE}$  decreased, consequently leading to decreases in the average refractive  $n_{av}$ .

These refractive indices can be attributed to the polarizabilities of atoms constituting the backbones of PSPIs moiety.<sup>1</sup> For PSPIs films, the number of  $CF_3$  groups increased with the increase in 6DFA content, consequently leading to decrease in refractive index of PSPIs. Thus, the lower refractive indices are attributed to the presence of bulky  $CF_3$  groups, which resulted in less efficient chain packing and low polarizability. The strong electronegativity of fluorine resulted in very low polarizability of the C—F bonds, thereby decreasing the dielectric constant. Thus with increase in  $CF_3$  groups, there is an increase in the number of polarizable atoms in a unit volume resulting in the decrease in polarizability and refractive index. In general, lower polarizability causes a lower dipole moment under electromagnetic field, providing a lower refractive index. The fluorine atom exhibits a relatively low polarizability and low index of refraction, because of its high electronegativity. Moreover, increases both in free volume due to bigger size of the  $CF_3$  groups and in interatomic repulsion of fluorine groups con-

tribute to the decrease in the net polarizability of the system. In general, the dielectric constant is proportional to the total polarization of the material including electronic, atomic, and dipolar polarizabilities.

### Morphological structure

Most of the polyimides are known to be an amorphous polymer. This may be due to its bulky and aromatic monomer and crosslinked arrangements of polymer chains.<sup>20–22</sup> The morphological structures of the PSPIs film were analyzed by X-ray diffractometry as shown in Figure 4. None of the polymers in the series showed any characteristic peak in the X-ray diffractogram of the well-defined long-range ordered structure or crystallinity as evident from the XRD data. All the polyimide films based on AHHFP and 6FDA exhibited broad peaks which indicated that the

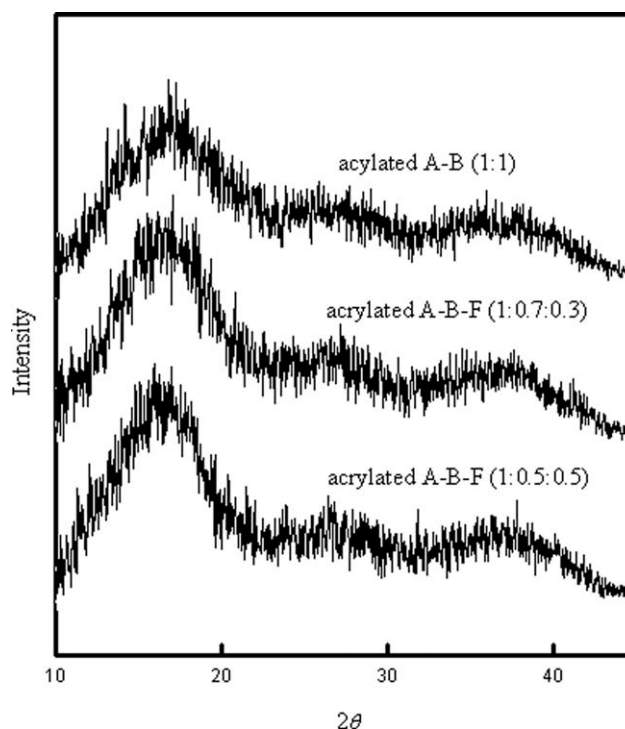


Figure 4 WAXD patterns of polyimide films.

polyimides were amorphous. This may be due to the presence of bulky  $\text{CF}_3$  which decreased the intra- and intermolecular interaction, resulting in loose polymer chain packing and aggregates and hinders the close packing between the polymer chains. The bulky  $\text{CF}_3$  groups also reduce attraction between molecules sterically. It can also confirmed that the intermolecular distance ( $d = 5.66 \text{ \AA}$ ) at the maximum amorphous halo peak ( $15.66^\circ$ ) of the AHHFP-BTDA-6FDA (1 : 0.5 : 0.5) is slightly bigger than that of the AHHFP-BTDA (1 : 1) which has  $5.22 \text{ \AA}$  of  $d$  value at the  $16.96^\circ$ . This indicates that the more bulky  $\text{CF}_3$  groups of the 6FDA expand the intermolecular distance and naturally form the more halo areas in the polymer chains. Further comparing the peaks of various PSPIs, the intensity and sharpness decreased with increasing the 6DFA moieties which indicates that, though the PSPIs films are structure-less, the molecular ordering decreased with increasing content of 6DFA moieties. These results well corresponds with the results of the dielectric constant measurement. With increase in the content of 6DFA moieties, the average refractive indices decreased, indicating the decreasing order in polymer chains.

### UV-vis analysis

The PSPIs were dissolved in DMAc with 10 mg of polymer in 1 mL of solvent. The solution put into quartz glass cell and measured by UV-vis spectrum analyzer. The UV-vis spectra of PSPIs are shown in Figure 5. The cutoff wavelengths ( $\lambda_{\text{cutoff}}$ ) of the films are in the range of 355–377 nm. The spectral shapes of the PSPIs are similar to each other and the transmittances of the film measured at 500 nm are higher than 70% in the visible region. The highest transparency of PSPIs is attributable to the bulky and twisted fluorine structures in the main chains which effectively weaken the intermolecular packing by increasing the free volumes among the PSPI chains. In addition, a secondary positive effect of the trifluoromethyl substituents on the film transparency is weakening of intermolecular cohesive force due to lower polarizability of the C–F linkage, and then reducing the formation of the interchain charge-transfer complex. The PSPIs absorb wavelength below 400 nm. This wavelength below 400 nm is well exposed at the low pressure mercury UV curing oven with 365–436 nm wavelengths. So this photosensitive polyimide could be used to photoresist.<sup>23</sup>

### Photosensitivity

PSPIs are an environmental improvement because of the reduction of organic solvents and associated volatile organic compounds. Photosensitive polyimides as photoimageable insulating materials make it pos-

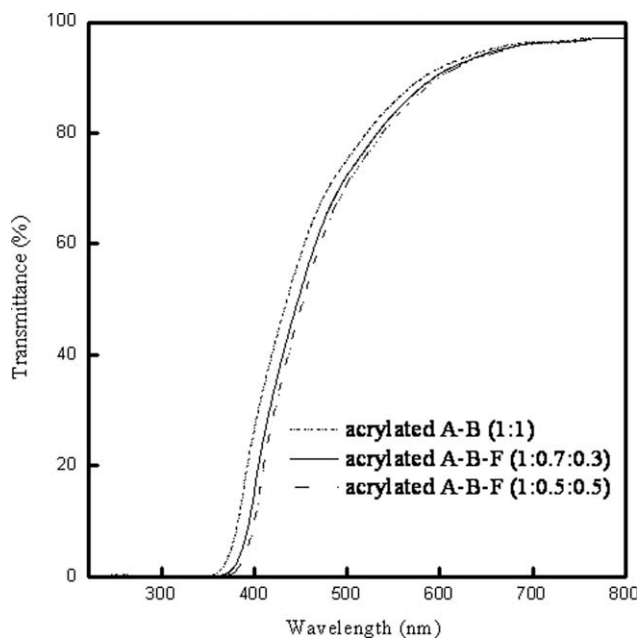


**Figure 5** UV-visible spectra of photosensitive polyimides.

sible for fine patterns to be formed with photolithography techniques, for underlying substrates to be protected, and for devices to be made resistant to heat and stress applied during subsequent processing, and they further simplify the complicated multi-step lithography processes. Therefore, interest in them has been growing for microelectronic applications such as interlayer dielectric and buffer coatings for semiconductor devices.

For negative-tone photoresist, the sensitivity is defined as the exposure dose required to effect 50% film thickness remaining after development. The lower the exposure dose is, the faster the photo speed is. Generally, there are lots of factors that affect the sensitivity of photopolymer—the photosensitive group, molecular weight, additives and so on. In our studies, the polymers all are the polyamic esters with acrylate as the photosensitive group. However, we found that the main chain structure of polymer and additives (such as sensitizer and photoinitiator) greatly affected the sensitivity of the photopolymer, but that the molecular weight of the polymer hardly affected the sensitivity.

The sensitivity curve for the negative-working film on a silicon wafer was obtained by the plotting of the normalized film thicknesses with  $2 \mu\text{m}$  remaining after development measured by surface profiler against the irradiated dose, as shown in Figure 6. The normalized film thickness was measured using the following equation.

Normalized film thickness

$$= \frac{\text{Thickness of an exposed film}}{\text{Thickness of exposed film}}$$

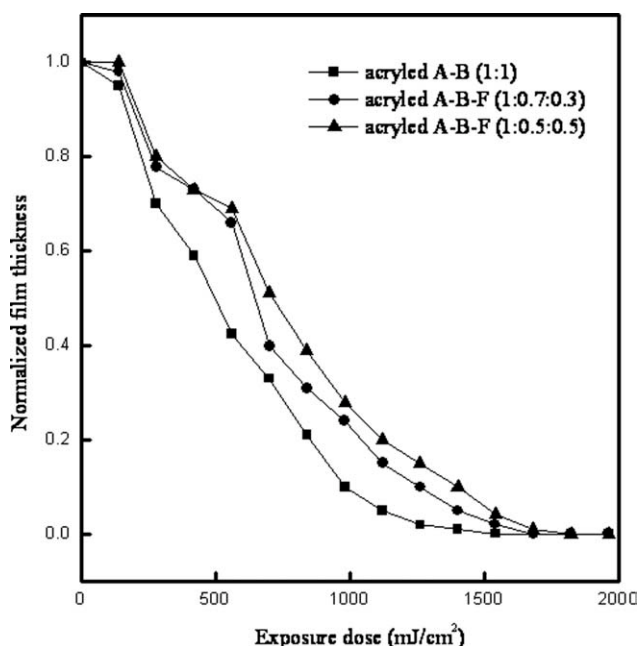


Figure 6 Photosensitivity of photosensitive polyimides.

The acrylated AHHFP-BTDA was the highest photosensitive than other PSPIs. It could be because structures in the polyimide chain can photolysis to produce several kinds of radicals, which can initiate polymerization of acrylate group to form crosslinking system. More containing BTDA had better photosensitivity. The photosensitivity are varied in the increasing order: Acrylated AHHFP-BTDA (1 : 1) > Acrylated AHHFP-BTDA-6FDA (1 : 0.7 : 0.3) > Acrylated AHHFP-BTDA-6FDA (1 : 0.5 : 0.5). This result represented the effect of BTDA amount in polyimide chain on the photosensitivity.

### Scanning electron microscope

Figure 7 shows the SEM images of the photosensitive acrylated AHHFP-BTDA (1 : 1) after UV expo-

sure and development by DMAc/2-propanol (volume ratio 5 : 1) for 3 min and rinsed with 2-propanol. The developed pattern sizes are 8  $\mu\text{m}$  and other shapes also formed well. It indicates that the PSPIs can play a decisive role in micro-scale photoresist.

### CONCLUSIONS

A series of new PSPIs were prepared by the polycondensation and further imidization of 2,2'-bis(3-amino-4-hydroxyphenyl)hexafluoropropane diamine (AHHFP) with 3,3',4,4'-benzophenonetetracarboxylic dianhydride (BTDA) and a mixture of various mole ratios of 3,3',4,4'-benzophenonetetracarboxylic dianhydride (BTDA) and 4,4'-(hexafluoroisopropylidene)diphthalic anhydride (6FDA). These polyimides exhibited excellent solubility in all the organic solvents of this study at room temperature. The glass transition temperatures ( $T_g$ s) of all PSPIs were more than 250°C as measured by DSC, and they exhibited good thermo-oxidative stability. The polymer films also showed high optical transparency, and low dielectric constants. Among the PSPIs, the acrylated AHHFP-BTDA-6FDA (1 : 0.5 : 0.5) has the lowest dielectric constants of 2.420 at 1 kHz and 2.170 at 1MHz by capacitance and optical methods, respectively. Morphology for all the PSPIs was confirmed by X-ray diffractions and SEM study. The photosensitivity (about 1400  $\text{mJ}/\text{cm}^2$ ) are varied as follows: acrylated AHHFP-BTDA (1 : 1) > acrylated AHHFP-BTDA-6FDA (1 : 0.7 : 0.3) > acrylated AHHFP-BTDA-6FDA (1 : 0.5 : 0.5). This result represented the effect of BTDA amount in polyimide chain on the photosensitivity. Finally, a pattern of 8 mm size was obtained from the acrylated AHHFP-BTDA (1 : 1). These results show that the PSPI may be a good material for potential applications such as high speed fine pattern semiconductor insulation layers, polarizer plates of liquid crystal display and are promising materials for optoelectric applications.

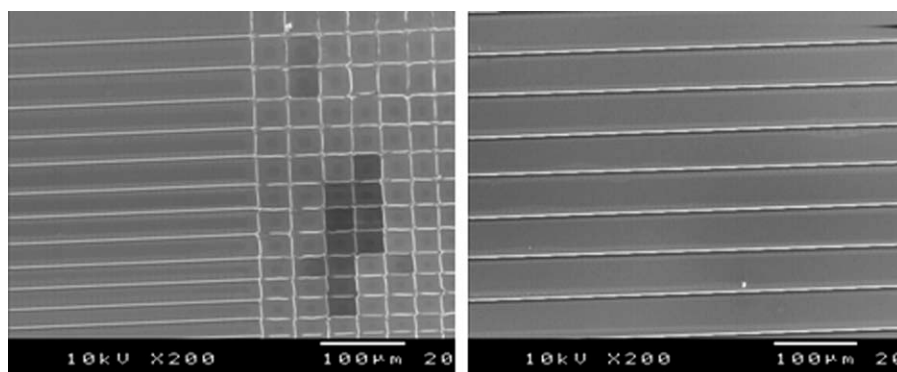


Figure 7 SEM of photosensitive polyimides patterning.



## References

1. Seo, J.; Jang, W.; Han, H. *J Appl Polym Sci* 2009, 113, 777.
2. Mochizuki, A.; Kurata, N.; Fukuoka, T. *J Photopolym Sci Technol* 2001, 4, 17.
3. Zhou, J. X.; Ishii, H. *J Appl Polym Sci* 2005, 98, 15.
4. Matsumoto, T. *J Photopolym Sci Technol* 2001, 14, 725.
5. Hsu, S. L.-C.; Fan, M. H. *Polymer* 2004, 45, 1101.
6. Jung, M.-S.; Joo, W.-J.; Choi, B.-K.; Jung, H.-T. *Polymer* 2006, 47, 6652.
7. Kim, K. H.; Jang, S.; Harris, F. W. *Macromolecules* 2001, 24, 8952.
8. Makita, S.; Kudo, H.; Nishikubo, T. *J Polym Sci Part A: Polym Chem* 2004, 42, 3697.
9. Jiang, X.; Li, H.; Wang, H.; Shi, Z.; Yin, J. *Polymer* 2006, 47, 2942.
10. Li, J.-S.; Li, Z.-B.; Zhu, P.-K. *J Appl Polym Sci* 2000, 77, 943.
11. Pyo, S. H.; Lee, M. Y.; Jeon, J. J.; Lee, J. H.; Yi, M. H.; Kim, J. S. *Adv Funct Mater* 2005, 15, 619.
12. Miyagawa, T.; Fukushima, T.; Oyama, T.; Iijima, T.; Tomoi, M. *J Polym Sci Part A: Polym Chem* 2003, 41, 861.
13. Seo, J.; Han, H. *Polym Degrad Stab* 2002, 77, 477.
14. Seo, J.; Han, H. *Polym Degrad Stab* 2001, 74, 133.
15. Chung, H.; Cho, K.-Y.; Han, H. *Polym J* 1999, 3, 700.
16. Chung, H.; Cho, K.-Y.; Han, H. *J Appl Polym Sci* 1999, 74, 3287.
17. Chen, C.; Qin, W.; Huang, X. *J Macromol Sci Part B* 2008, 47, 783.
18. Lee, C.; Shul, Y.; Han, H. *J Polym Sci Part B: Polym Phys* 2002, 40, 2190.
19. Lin, C. H.; Jiang, Z. R.; Wang, C. S. *J Polym Sci Part A: Polym Chem* 2002, 40, 4084.
20. Mathakari, N. L.; Jadhav, V. S.; Kanjilal, D.; Bhoraskar, V. N.; Dhole, S. D. *Surf Coat Technol* 2009, 203, 2620.
21. Maji, S.; Sen, S. K.; Dasgupta, B.; Chatterjee, S.; Banerjee, S. *Polym Adv Technol* 2009, 20, 384.
22. Yan, J.; Wang, Z.; Lv, C.; Yang, H.; Shang, Z.; Gao, L.; Ding, M. *J Appl Polym Sci* 2008, 110, 706.
23. You, N. H.; Suzuki, Y.; Yorifuji, D.; Ando, S.; Ueda, M. *Macromolecules* 2008, 41, 6361.